Desalination and Water Treatment
www.deswater.com
doi: 10.1080/19443994.2015.1089195

57 (2016) 18560–18571
August

Taylor & Francis
Taylor & Francis Group

Preparation and characterization of polypropylene fiber-grafted polybutylmethacrylate as oil sorbent

Wenbo Chai[a], Xiaoyan Liu[a,*], Xinying Zhang[a,b,*], Beibei Li[a], Tiantian Yin[a], Junchen Zou[a]

[a]*College of Environmental and Chemical Engineering, Shanghai University, 99 Shangda Road, Shanghai 200444, P.R. China, Tel. +1 8818215695; email: chaiwenbo1988@163.com (W. Chai), Tel. +86 21 66137767; Fax: +86 21 66137761; emails: lxy999@shu.edu.cn (X. Liu), Tel. +86 18818216331; email: zhangxinying008@163.com (X. Zhang), Tel. +86 13816220295; email: 743421914@qq.com (B. Li), Tel. +86 15036065609; email: 1073047772@qq.com (T. Yin), junchen526@163.com (J. Zou)*
[b]*College of Materials Science and Engineering, Shanghai University, 99 Shangda Road, Shanghai 200444, P.R. China*

Received 19 December 2014; Accepted 26 August 2015

ABSTRACT

Polypropylene fiber-grafted polybutylmethacrylate (PP-g-PBMA), a new oil absorbent, was prepared by suspension polymerization using butyl methacrylate as monomer, benzoyl peroxide (BPO) as initiator, and N,N´-methylenebisacrylamide as cross-linker. The effects of monomer concentration, initiator concentration, and cross-linker dosage on the oil absorbency were studied. The results revealed that the pseudo-second-order kinetics model fitted well with the experimental results. The sorption isotherms studies indicated that the equilibrium process was well described by the Freundlich isotherm model. The structures of polypropylene fiber (PP) and PP-g-PBMA were characterized by Fourier transform infrared (FTIR) spectroscopy, scanning electron microscopy (SEM), N_2 adsorption–desorption, contact-angle (CA) measurements, and differential thermogravimetric analysis. The results of FTIR and SEM show that PBMA was successfully grafted onto PP fiber substrate. The maximum oil sorption capacity of PP-g-PBMA for toluene, diesel, soybean oil, and lubricating oil can reach 18.65, 25.74, 33.56, and 38.90 g/g, respectively. In order to simulate real marine environment, the oil sorption capacities of PP-g-PBMA at different stirring speed values, temperatures, and salinity were investigated. Furthermore, PP-g-PBMA can be reused and recycled more than eight times. It can be concluded that PP-g-PBMA with low-cost and high oil sorption capacity could be used for removal of oil spill.

Keywords: Polypropylene fiber; Polybutylmethacrylate; Suspension polymerization; Oil sorption capacity; Reusability

1. Introduction

Nowadays the accidents of oil spill or organic pollutants can cause damage to animals, human beings, and environment which had attracted more and more attention by many researchers [1–4]. The existing methods for removal of oily wastewater include *in situ* burning, mechanical extraction, bioremediation, sorbents, etc. However, among these existing techniques for removal of oil pollution, the use of sorbents is generally considered to be a simple,

*Corresponding authors.

efficient, and environment-friendly way because of their rapid removal efficiency and good recycling capability [5–7]. Oil sorbents can be classified into three major groups: inorganic materials, natural materials, and organic synthetic polymers [8]. The inorganic materials include fly ash [9,10], expanded perlite [11,12], silica aerogels [13], etc. Natural fiber materials, such as barley straw [14–16], populus seed fibers [17], banana fibers [18,19], and kapok fibers [20,21], have been investigated. Synthetic polymers, such as polyacrylonitrile [22] and polyurethane [23], have been used for oil spill cleanup because of their rapid oil sorption rate and hydrophobic properties.

In a general way, an ideal sorbent would be have the properties of high uptake capacity, fast oil absorption rate, good buoyancy, high selectivity for oil and water, low cost and good recycling ability [24]. An attractive candidate for removal of oil pollution may be the low-cost materials [25]. In this case, one of the synthetic fibers, polypropylene (PP) fibers were low-cost materials with the advantages of low density, rapid sorption rate, oleophilic properties, and simply fabrication reported by some researchers [26,27]. This implies that PP fibers are potential oil sorbents. Furthermore, base on PP fibers, some novel oil sorbents were prepared by melt electrospinning method [28], melt blown method [29], chemical vapor deposition method [30], and ultraviolet method [31].

Polymerization is a simple and effective method to graft monomers onto fiber surface. This method is widely used by researchers [32–34]. In this study, polypropylene fiber-grafted polybutylmethacrylate (PP-g-PBMA) was prepared by suspension polymerization using MBA as monomer, benzoyl peroxide (BPO) as initiator and N,N-methylene-bis-acrylamide as cross-linker. The aims of this work were to (1) enhance the oil sorption capacity of PP fiber through the surface modification, and (2) evaluate the effects of preparation variables and environment conditions on the oil absorbency of PP-g-PBMA.

2. Materials and methods

2.1. Materials

PP fiber (fiber diameter = 18–20 μm, density = 0.91 g/cm^3) was purchased from Shanghai Ying-Jia Industrial Development Co. Ltd, China. BMA (chemically pure) and BPO (chemically pure) were provided by Shanghai Sinopharm Chemical Reagent Co. Ltd, China. N,N´-methylenebisacrylamide (99%) was supplied by Aladdin Chemistry Co. Ltd, Shanghai, China. Nitrogen (the purity exceeds 99.99%) was received from Shanghai Tomoe Gases Co. Ltd, China. All other chemical reagents from Shanghai Sinopharm Chemical Reagent Co. Ltd, were of analytical grades. The properties of toluene, diesel, soybean oil, and lubricating oil are displayed in Table 1.

All the chemical reagents were used without further purification except for MBA and BPO. To remove the inhibitor in the MBA, firstly, it was washed by 5% aqueous sodium hydroxide, and then dried by anhydrous $CaCl_2$ for 3 h, finally the purified MBA was collected by vacuum distillation. BPO was purified using chloroform and methanol. Purified MBA and BPO were kept in different brown bottles for further use.

2.2. Preparation of PP-g-PBMA oil sorbent

The deionized water (100 mL) was placed in a four-necked round-bottom flask (250 mL), and then a mechanical stirrer and a reflux condenser were fixed on the flask. The PP fiber (1 g) was dispersed to 100 mL of deionized water with 200 rpm agitation. Then the reaction liquid was heated to 70℃ under a flow of nitrogen in an oil bath and maintained for 10 min. Afterward, MBA (0.1–0.7 M), BPO (0.5–2.0 mM), and N,N´-methylenebisacrylamide (0.1–3.0%) were added into the flask. Here, the percentage of N,N´-methylenebisacrylamide stands for the ratio of cross-linker (g) to PP fiber (g). After being kept for 6 h, the flask was withdrawn from the oil bath and the products were taken out. The grafted PP fiber was washed with the solvents in the following sequence for three times: acetone, ethanol and deionized water, and then dried in a vacuum oven at 70℃ for 16 h. After being dried, the products were extracted with toluene (150 mL) for 48 h in a soxhlet extractor, and then thoroughly rinsed with 60–80℃ hot deionized water and 95% ethanol. Finally, the products were dried in a vacuum oven at 70℃ overnight and put in a desiccator.

2.3. Characterization

The Fourier transform infrared (FTIR) spectra of PP and PP-g-PBMA were collected on a FTIR spectrometer

Table 1
Physical properties of studied oils at room temperature

Oil type	Density (g/cm^3)	Viscosity (mm^2/s)
Toluene	0.866	0.677
Diesel	0.82	6.51
Soybean oil	0.93	7.26
Lubricating oil	0.88	47–57

(Nicolet 380, Thermo Fisher Scientific, USA) using KBr pellets in the range of 400–4,000 cm^{-1}. The analysis of surface morphology was performed using scanning electron microscope (SEM, SU-1510, Hitachi Ltd, Japan) at room temperature. For SEM study, the samples were coated with gold and images were recorded at an accelerating voltage of 20 kV. The surface areas, pore volumes, and pore sizes of PP and PP-g-PBMA were measured using a surface analyzer (ASAP 2020, Micromeritics Ltd, USA) by Brunauer–Emmett–Teller (BET) method. The samples were degassed at 100˚C in a N_2 atmosphere. Contact angle (CA) measurements were performed using drops of distilled water or diesel oil (5 μL) at room temperature (OCA30, Dataphysics, Germany). The average value was obtained by three measurements at different positions on the sample. Differential thermogravimetric analysis (DTG) of PP and PP-g-PBMA was conducted under a nitrogen atmosphere from room temperature to 600˚C at a heating rate of 10˚C/min (STA 499 C, Netzsch Ltd, Germany).

2.4. Oil absorption capacities

A total of 0.1 g dried sample with a stainless steel wire mesh (weighed before sorption) was added into 300-mL pure oil in a 500-mL glass beaker. After 15 min, the sample and wire mesh were removed from the oil and held to drain for 5 min. Finally, the oil absorbing material was weighed in a digital balance (1×10^{-4} g accuracy). The oil sorption capacity of the sample was evaluated by Eq. (1).

$$Q = \frac{m_o - m_d - m_a}{m_d} \quad (1)$$

where Q is oil sorption capacity of the sample (g/g); m_o and m_d are the weight of the oil-loaded sample after 5 min of drainage (g) and the dry sample (g), respectively; and m_a is the weight of absorbed water.

The same procedure was conducted for kinetic study. The material was picked up at different time intervals (0, 5, 10, 20, 30, 60, 120, 180, 300, 600, 900 s). The calculations were similarly performed. All the experiments were repeated thrice under identical conditions and the standard deviations were measured.

2.5. Effect of environment conditions on the oil absorbency

A series of experiments were performed in 500-mL glass beaker containing 300 mL of artificial seawater and 100 mL of oil. The artificial seawater was prepared by adding sodium chloride into deionized water. For example, 30 g of sodium chloride was dispersed into 970 mL of water, and then 30% of artificial seawater can be obtained. In order to evaluate the effect of stirring speed on oil uptake, 0.1 g of sample was added into the mixture (salinity 30%) for 15 min at 25˚C, the oil sorption capacities were obtained at different stirring speed (0, 24, 48, 96, 144, and 192 rpm). In order to investigate the effect of seawater temperature on oil sorption capacity, 0.1 g of sample was added into the mixture (salinity 30%) for 15 min with a constant speed of 96 rpm at different temperature levels (5, 15, 25, 35, and 45˚C). In order to examine the effect of salinity on the oil absorbency, and 100 mL of oil, 0.1 g of sample was added into the mixture with different salinity (0, 10, 20, 30, and 40%) for 15 min with a constant speed of 96 rpm at 25˚C.

2.6. Test of reusability

Reusability test was performed in oil/water mixture for 15 min at room temperature by adding 0.1 g of dried sample with a stainless steel wire mesh into 500-mL glass beaker containing 300 mL of water and 100 mL of oil. After the first sorption test, the oil-saturated sample was removed from the mesh and the oil was recovered by the help of a vacuum pump. Then the sample was measured and reused in the next adsorption–desorption test. The above method was applied for eight cycles and the oil absorbency of the material after each cycle was obtained.

3. Results and discussion

3.1. Effects of preparation parameters on the oil absorbency

3.1.1. Effect of monomer concentration

The changes of the oil sorption capacity with the monomer concentration are shown in Fig. 1(a). The oil sorption capacity is the maximum at the monomer concentration of 0.5 M. The oil sorption capacity for diesel gradually increases when the monomer concentrations increase from 0.1 to 0.5 M. However, further increasing the monomer concentration will lead to decrease in oil absorbency. This may be due to the fact that an excess of monomer cannot be initiated and the graft polymerization reaction will be inhibited by the self-polymerization of excess monomer [31,32]. The results suggest that monomer concentration has an important influence on the oil absorbency.

3.1.2. Effect of initiator concentration

The effect of initiator concentration on oil sorption capacity is shown in Fig. 1(b). As depicted in Fig. 1(b),

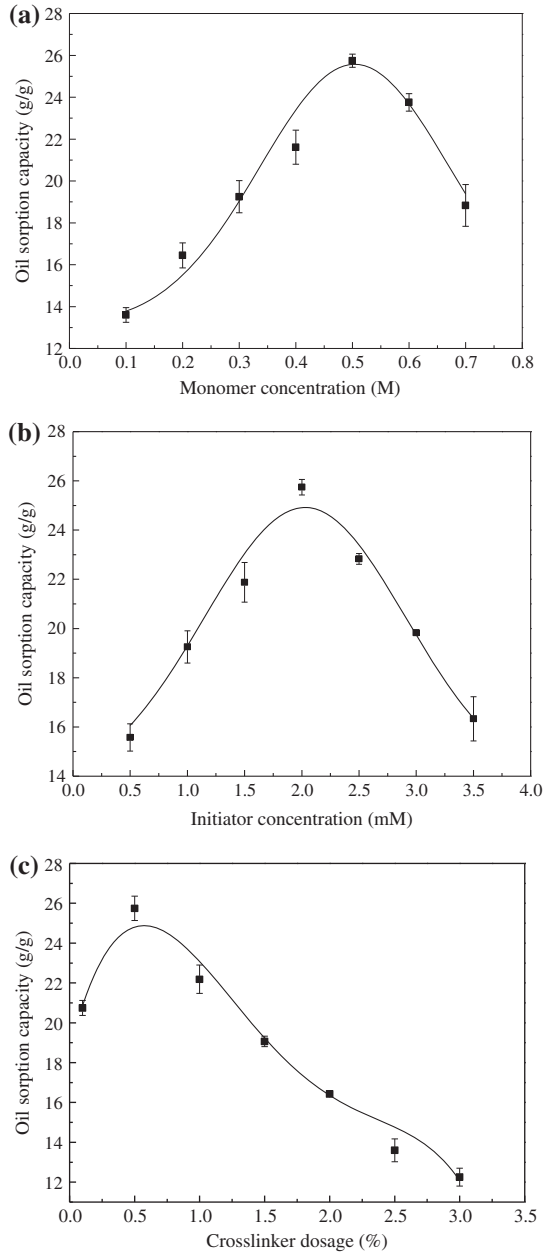

Fig. 1. Effect of different variables on oil sorption capacity. (a) Monomer concentration (initiator concentration: 2.0 mM, cross-linker dosage: 0.5%), (b) initiator concentration (monomer concentration: 0.5 M, cross-linker dosage: 0.5%), and (c) cross-linker dosage (monomer concentration: 0.5 M, initiator concentration: 2.0 mM).

the oil sorption capacity continuously increases with the initiator concentration ranging from 0.5 to 2.0 mM, then decrease with further increase in the initiator concentration. The oil sorption capacity can reach 25.74 g/g at 2.0 mM initiator concentration. Previous study demonstrated that the initiator concentration played an important role on the size of polymer chains because it can affect the properties of oil-absorbent by generating free radical [35]. It is difficult to generate sufficient free radical to initiate more active sites on monomer molecule under the lower initiator concentration. The formation of polymer chains may be affected. On the contrary, the higher concentration of initiator would accelerate the termination of graft polymerization reaction, which led to the decrease in the polymer chains in the network.

3.1.3. Effect of cross-linker dosage

To understand the effect of cross-linker dosage on oil sorption capacity for diesel, batch experiments were conducted at different cross-linker levels (0.1, 0.5, 1.0, 1.5, 2.0, 2.5, and 3.0%). With the increase in cross-linker dosages, oil sorption capacity firstly increases and then significantly decreases with cross-linker dosage increasing from 1.0 to 3.0%, as illustrated in Fig. 1(c). Cross-linking density is also an important factor for improving oil sorption capacity of material [35]. An appropriate cross-linker dosage can generate a good three-dimensional network, which is favorable for retaining oil. However, the network generating with low-cross-linker dosage is easy to collapse, which results in the lower oil absorbency. In addition, an excess of cross-linker is unfavorable for holding oil because the three-dimensional network is more compact.

3.2. Characterization

3.2.1. FTIR spectra analysis

The FTIR spectra of PP and PP-g-PBMA are displayed in Fig. 2. Firstly, an increase in the intensity of the absorption peaks can be found around 2,965, 1,459 and 1,376 cm^{-1}, which are ascribed to C–H stretching vibration in CH_3, C–H bending vibration in CH_2 and CH_3, respectively. A new absorption peak appears at 1,720 cm^{-1} corresponding to stretching vibration of carbonyl group (C=O) in PP-g-PBMA, suggesting that PMBA had been successfully grafted onto the surface of PP.

3.2.2. SEM analysis

SEM images of PP and PP-g-PBMA are shown in Fig. 3. From Fig. 3(a) and (b), it can be seen that PP shows a smooth surface and tubular structure. The smooth surface is unfavorable for holding oil. In comparison, an undulant and corrugated structure can be

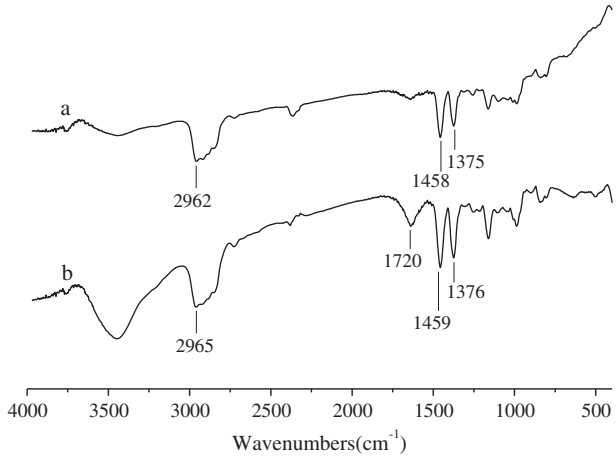

Fig. 2. FTIR spectra of (a) PP and (b) PP-g-PBMA.

seen on the images of PP-g-PBMA (Fig. 3(c) and (d)), which facilitates the penetration of oil. There is rougher surface on PP-g-PBMA than PP (Fig. 3(c) and (d)). The rougher surface increases the surface area of the material, which can prevent absorbed oil escaping from the surface. Thus, the oil sorption capacity of the material was improved.

3.2.3. BET analysis

Nitrogen sorption measurements were performed to further investigate the pore parameter of the adsorbents. The surface areas, pore volumes, and pore sizes of PP and PP-g-PBMA were measured by N_2 adsorption–desorption isotherms. Nitrogen adsorption–desorption isotherms of PP and PP-g-PBMA are shown in Fig. 4. In accordance with the IUPAC classification, the adsorbents showed a typical type II adsorption–desorption isotherm, indicating the presence of mesopores (2–50 nm pore width) [36]. As shown in Table 2, the surface areas of PP and PP-g-PBMA were 1.58 and 6.15 m^2/g, respectively. The pore sizes of PP and PP-g-PBMA were 0.37 and 2.83 nm, respectively. The results indicated that the modification with PBMA could increase the surface area and pore volume of PP. This may be that graft polymerization induced the highest specific surface area coupled with hydrophobicity and surface roughness. In order to investigate the wettability of PP and PP-g-PBMA, the CA measurements were carried out for further observation.

3.2.4. CA measurements

CA measurements for distilled water and diesel oil droplets on dry samples at room temperature are

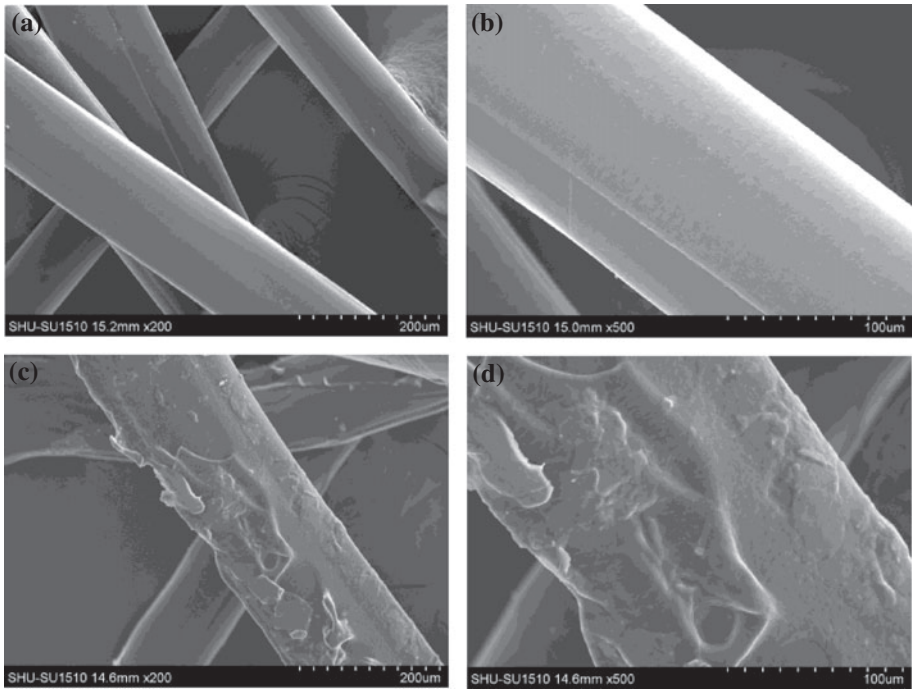

Fig. 3. SEM images of PP at (a) low magnification (200×) and (b) high magnification (500×), PP-g-PBMA at (c) low magnification (200×) and (d) high magnification (500×).

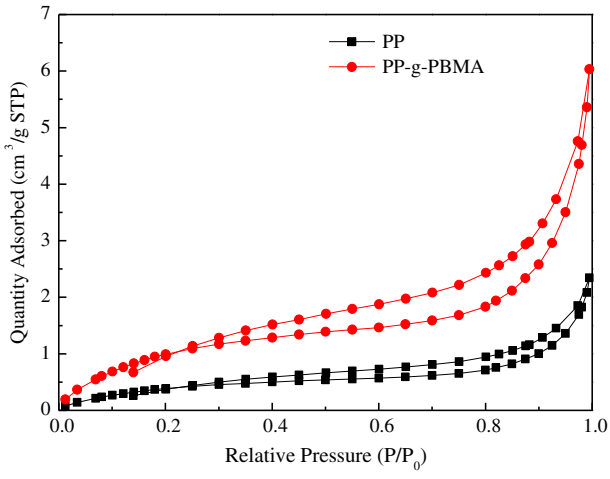

Fig. 4. Nitrogen adsorption–desorption isotherms of PP and PP-g-PBMA.

shown in Fig. 5. As depicted in Fig. 5(a), the water contact angle of PP was only 90.3°, while the CA of PP-g-PBMA could reach 123.9° (Fig. 5(b)), and the water droplet of PP-g-PBMA kept the spherical shape until it dried. Moreover, an oil droplet could immediately spread on the surface of PP-g-PBMA and rapidly penetrate into the sorbent in less than 1 s, and the oil contact angle was 0° (Fig. 3(c–e)), showing hydrophobic and oleophilic characteristics. Generally, roughness and low surface energy contributed to the superhydrophobicity [37]. So the surface roughness of PP increased by graft polymerization method.

3.2.5. DTG analysis

The thermal stabilities of PP and PP-g-PBMA were investigated by DTG from room temperature to 600℃. The DTG curves of PP and PP-g-PBMA were presented in Fig. 6. As illustrated in Fig. 6, an obvious mass loss was detected at the temperature of 400–500℃ (about 450℃), and this significant loss may be attributed to decomposition of polypropylene fiber matrix. Gwon et al. reported that PP is completely degraded before the temperature reaching around 460℃ [38]. The TGA curve of PP-g-PBMA was similar to the TGA curve of PP fiber. The mass loss in the temperature range of 390−410℃ was slight larger due to decomposition of butyl methacrylate (BMA) chain. The results indicated that graft polymerization had no significant effect on the decomposition temperature of the polypropylene matrix.

3.3. Oil adsorption experiments

3.3.1. Comparison of PP and PP-g-PBMA in different oils

The oil sorption capacities of PP and PP-g-PBMA for toluene, diesel, soybean oil, and lubricating oil are

Table 2
BET surface areas, pore volumes, and pore sizes of PP and PP-g-PBMA

Sample	BET surface area (m^2/g)	Pore volume (cm^3/g)	Pore size (nm)
PP	1.58	0.0011	0.37
PP-g-PBMA	6.15	0.0127	2.83

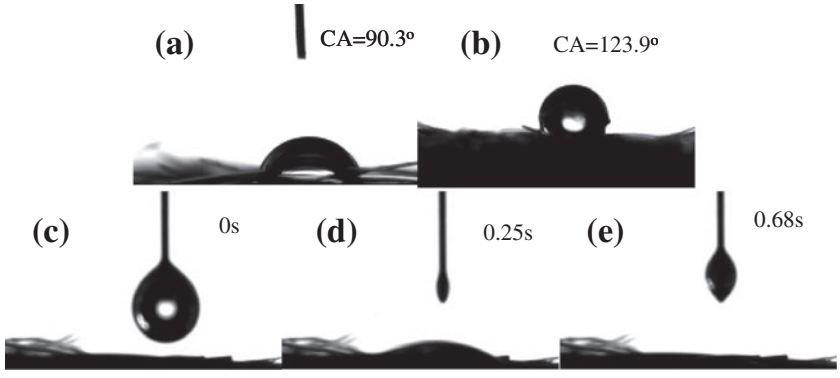

Fig. 5. CA measurements of a water drop on the surface of (a) PP, and (b) PP-g-PBMA. Time-dependent images of diesel oil droplets (c–e) absorbed by PP-g-PBMA at room temperature.

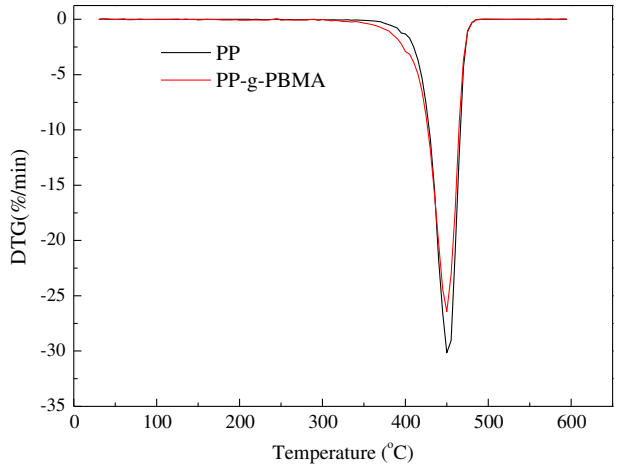

Fig. 6. DTG curves of PP and PP-g-PBMA measured in a nitrogen atmosphere.

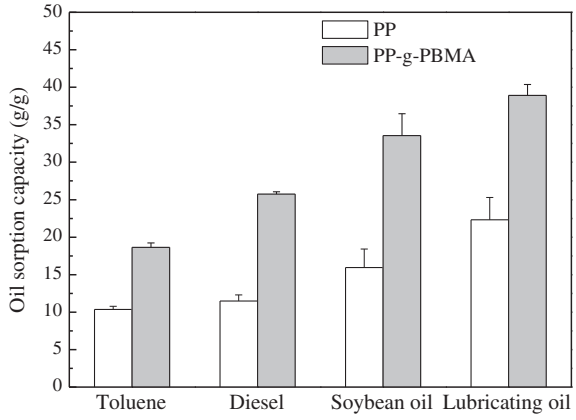

Fig. 7. Oil sorption capacity of PP and PP-g-PBMA in different kinds of oils.

illustrated in Fig. 7. The oil sorption capacity of PP for toluene, diesel, soybean oil, and lubricating oil is 10.36, 11.43, 15.93, and 22.32 g/g, respectively. By contrast, the oil sorption capacity of PP-g-PBMA for above four oils can reach 18.65, 25.74, 33.56, and 38.90 g/g, respectively. This result indicates that oil sorption capacities of PP-g-PBMA are significantly improved by surface modification. After surface modification, the fibers become rough and the rough surface is beneficial for retaining oil. In comparison, the absorbed oil can easily escape from the smooth surface of PP. Besides, the as-prepared PP-g-PBMA shows higher toluene absorbency than other oil-absorbing polymers previously published (Table 3), which indicates that PP-g-PBMA used for removing oil is more efficient and effective.

3.3.2. Adsorption kinetic

Adsorption kinetic study is one of important characteristics for depicting the sorption rate. Rapid oil sorption rate will be more attractive for removal of actual oil spill. Effects of contact time on the oil absorbency of PP-g-PBMA for three oils are displayed in Fig. 8. It can be observed that PP-g-PBMA shows a fast adsorption rate for three types of oils during the initial 20 s, and the saturated oil adsorption capacity can be reached within 5 min. The oil sorption capacity of lubricating oil for PP-g-PBMA is much higher than those of diesel and soybean oil. This may be attributed to the high viscosity of lubricating oil. The high viscosity can enhance the adherence of oil onto the sorbent surface, leading to an increase in oil sorption capacity [41]. In addition, the sorption capacities for diesel, soybean oil, and lubricating oil are in agreement with the trends of oil viscosity.

In order to determine relevant parameters, batch kinetic data obtained were processed in conjunction with appropriate models mentioned in the literature [42]. In this connection, both the pseudo-first-order and the pseudo-second-order adsorption kinetic models are presented in the following. The pseudo-first-order adsorption kinetics can be described as:

$$\frac{dq}{dt} = k_1(q_e - q_t) \tag{2}$$

where q_e is the equilibrium amount of adsorbed contaminant (g) per unit mass (g) of the adsorbent, q_t is

Table 3
Comparison of toluene absorbency from this work and other polymers

Oil-absorbing polymers	Toluene absorbency (g/g)	Refs.
Polybutylmethacrylate/kapok fiber	14.6	[32]
Poly(methyl methacrylate–butyl methacrylate) resins	17.6	[39]
Commercial polypropylene Methacrylate–lauryl methacrylate fiber	15	[40]
PP-g-PBMA	18.7	This work

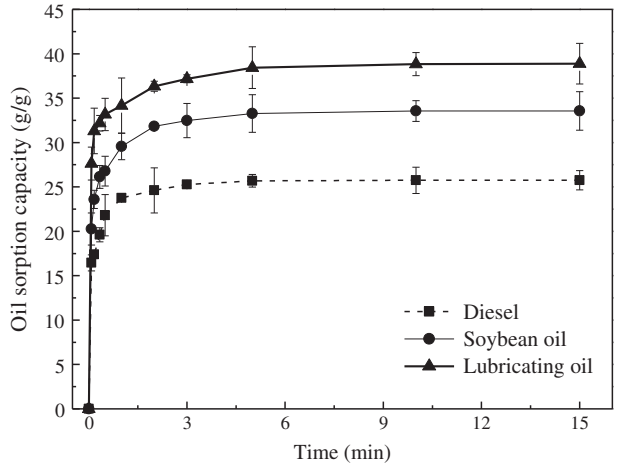

Fig. 8. Adsorption kinetic curves of PP-g-PBMA for diesel, soybean oil, and lubricating oil.

adsorbed amount at any time t, and k_1 is the first-order rate constant (1/min). Integrating the above equation with the limit $q = 0$ at time $t = 0$ gives:

$$\ln \frac{q_e - q_t}{q_e} = -k_1 t \tag{3}$$

Eq. (3) can also be rewritten as:

$$\ln (q_e - q_t) = -k_1 t + \ln q_e \tag{4}$$

It is clear from Eq. (4) that a plot of $\ln (q_e - q_t)$ vs. time yields a straight line of slope $-k_1$ and the y-intercept as $\ln (q_e)$.

On the other hand, the pseudo-second-order adsorption kinetics is represented as:

$$\frac{dq}{dt} = k_2 (q_e - q_t)^2 \tag{5}$$

Here, k_2 is the pseudo-second-order rate constant (g adsorbent per g contaminant per min). The integration of Eq. (5) with the limit $q = 0$ at time $t = 0$ gives:

$$\frac{1}{q_e - q_t} - \frac{1}{q_e} = -k_2 t \tag{6}$$

Rearrangement of the above equation yields:

$$\frac{t}{q_t} = \frac{t}{q_e} + \frac{1}{k_2 q_e^2} \tag{7}$$

Therefore, a plot of (t/q_t) vs. time yields a straight line with the slope of $(1/q_e)$ and the y-intercept of $(k_2 q_e^2)^{-1}$.

The results of R^2 represent the fitting correlation coefficient obtained from the models of diesel, soybean oil, and lubricating oil, respectively, as shown in Table 4. Also, Table 4 presents the other relevant parameters of sorption. From Table 4, it can be seen that the fitting results for the pseudo-second-order kinetic equation are superior to the pseudo-first-order kinetic equation in describing the adsorption of oil/water mixture for PP and PP-g-PBMA. So the sorption can be described as chemisorption [43].

3.4. Equilibrium sorption isotherms

It is very practical for equilibrium adsorption isotherm studies which can describe the adsorption properties of sorbents. Batch isotherm experiments were conducted in oil/water mixture at different temperature (20, 25, and 30°C). The concentrations of

Table 4
Kinetic parameters of pseudo-first-order models and pseudo-second-order models on PP and PP-g-PBMA

Sample	Oil type	Kinetics	R^2	q_e	Rate constant
PP	Diesel	First-order	0.9254	0.68	0.0039
		Second-order	0.9998	11.21	0.0403
	Soybean oil	First-order	0.8156	3.88	0.0037
		Second-order	0.9996	15.80	0.0272
	Lubricating oil	First-order	0.9587	9.35	0.0069
		Second-order	0.9999	22.05	0.0517
PP-g-PBMA	Diesel	First-order	0.9158	5.87	0.0026
		Second-order	0.9995	25.08	0.0208
	Soybean oil	First-order	0.9265	6.72	0.0086
		Second-order	1.0000	33.21	0.0358
	Lubricating oil	First-order	0.9352	10.06	0.0057
		Second-order	0.9989	38.66	0.0086

diesel oil used varied from 0.02 to 0.12 g/mL of water at 150 rpm.

In this study, two models were applied for the equilibrium data of PP-g-PBMA: Langmuir and Freundlich isotherms. Langmuir adsorption model [44] assumes that adsorption occurs at specific homogeneous adsorption sites within the adsorbent and intermolecular forces decrease rapidly with the distance from the adsorption surface. The model further based on the assumption that all the adsorption sites are energetically identical and adsorption occurs on a structurally homogeneous adsorbent. Langmuir model which has been successfully applied to many sorption processes is:

$$q_e = \frac{q_0 b C_e}{1 + b C_e} \tag{8}$$

The linear form of Langmuir isotherm is expressed as:

$$\frac{1}{q_e} = \frac{1}{q_0} + \frac{1}{b q_0 C_e} \tag{9}$$

wherein q_e is amount of diesel sorbed at equilibrium per unit mass of sorbent (mg/g) and C_e is the equilibrium concentration of diesel in solution (mg/L). The constant q_0 signifies the maximum sorption capacity (mg/g) and b is related with the energy of the adsoprtion (L/mg). The essential characteristics of Langmuir isotherm can be expressed in terms of a dimensionless constant separation factor R_L that is given by Eq. (10) [45]:

$$R_L = \frac{1}{1 + b C_0} \tag{10}$$

wherein C_0 is the highest initial concentration of sorbate (mg/L), and b (L/mg) is the Langmuir constant. The value of R_L indicates the type of the isotherm to be either unfavorable ($R_L > 1$), linear ($R_L = 1$), favorable ($0 < R_L < 1$), or irreversible ($R_L = 0$).

The Freundlich isotherm is an empirical equation employed to describe heterogeneous systems. The Freundlich equation is expressed as:

$$q_e = K_F C_e^{\frac{1}{n}} \tag{11}$$

wherein K_F and n are the Freundlich constants with n giving an indication of how favorable the adsorption process is. The magnitude of the exponent, $1/n$, gives an indication of the favorability of adsorption. Values of $n > 1$ represent favorable adsorption condition [46]. Eq. (12) may be written in the logarithmic form as:

$$\ln q_e = \ln K_F + \frac{1}{n} \ln C_e \tag{12}$$

The isotherm constants for all the isotherms studied, and the correlation coefficient, R^2 with the experimental data are listed in Table 5. In view of the values of linear regression coefficients and the oil sorption capacity in Table 5, Freundlich models exhibited better fit to the sorption data of PP-g-PBMA than Langmuir models in the studied initial concentration range.

3.5. Effect of environment conditions on the oil sorption capability

3.5.1. Stirring speed

Stirring speed is an important factor for oil removal from water surface. The stormy waves in different locations are not the same. In order to simulate the size of stormy waves, different stirring speed values are chosen to investigate the oil absorbency by PP-g-PBMA. The oil sorption capacities of PP-g-PBMA for diesel, soybean oil, and lubricating oil at different stirring speed values are shown in Fig. 9(a). The oil sorption capacity increases with the stirring speed increasing from 0 to 96 rpm, but significantly decrease with further increase in the stirring speed. In oil/water mixture, the maximum sorption capacities of PP-g-PBMA for diesel, soybean oil, and lubricating oil can reach 25.09, 32.46, and 37.70 g/g at 96 rpm, respectively. When the stirring speed was too low, the oil molecules cannot be fully contacted with sorbent. As a result, the oil sorption capacity was not so encouraging. Increasing the stirring speed would be beneficial for the sorption process because Brownian motion accelerated and more oil molecules were attached the surface of sorbent. However, the higher stirring speed was unfavorable for sorption that too fast movement of oil molecules may be decrease the

Table 5
Parameters of Langmuir and Freundlich model constants and correlation coefficients for sorption of diesel with PP-g-PBMA

T (℃)	Freundlich			Langmuir		
	R^2	n	K_f	R^2	q_0	b
20	0.9211	0.2891	14.9899	0.7949	26.0417	0.0207
25	0.9446	0.2832	13.3690	0.8848	24.2718	0.0286
30	0.9210	0.3071	11.1867	0.8408	21.6920	0.0386

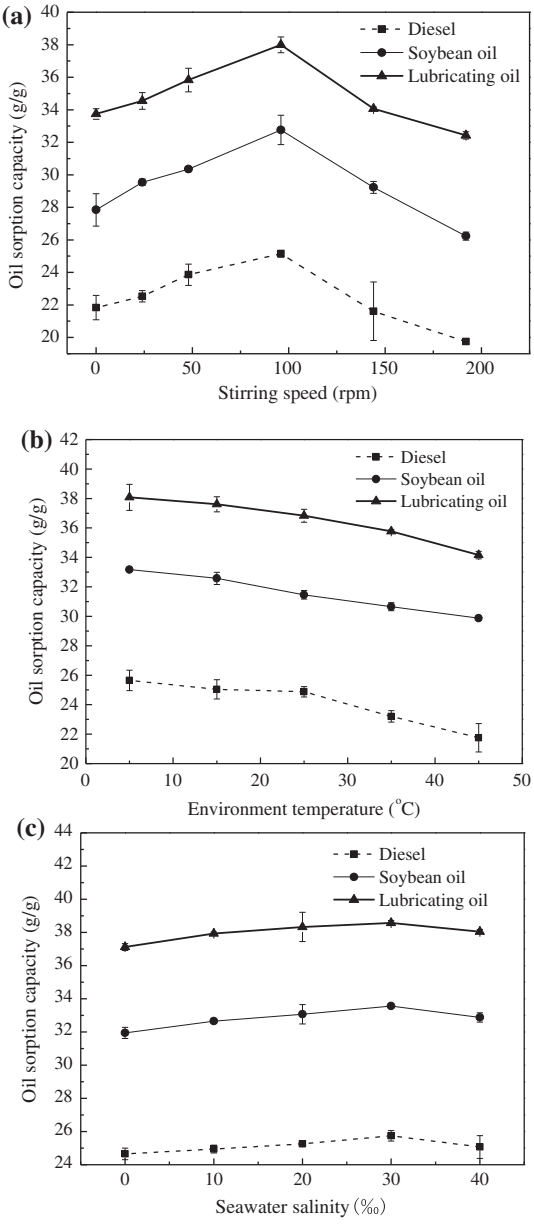

Fig. 9. Effect of (a) stirring speed, (b) environment temperature, and (c) seawater salinity on oil sorption capacity by PP-g-PBMA.

chance that was absorbed by the material. Therefore, if the stormy waves were too large, this will be an adverse impact on the adsorption. The optimum stirring speed (96 rpm) was used for following experiments.

3.5.2. Environment temperature

Environment temperature is also an important factor which had been investigated by some researchers [47–49] because accidental oil pollution may occur in different seasons. Fig. 9(b) shows the influence of the environment temperature on the oil sorption capacity by PP-g-PBMA. With temperature increasing from 5 to 45℃, the oil sorption capacity gradually decreases. Therefore, high temperature is unfavorable for oil sorption and sorption process may be exothermic. High temperature can accelerate the movement of oil molecules. High temperature can also lead to a decrease in oil viscosity. Low viscosity made the oil harder to adhere to the fiber surface [50], resulting in the decrease in oil sorption capacity.

3.5.3. Seawater salinity

The salinity in deep sea, coast, and river is different. In the estuary sea area near the river, the salinity is sharply decreased. In general, the water salinity in deep sea can reach 35%. In this study, the maximum salinity was chosen as 40%. Effect of the salinity on the oil sorption capacity is displayed in Fig. 9(c). It can be observed that salinity has a negligible impact on the oil sorption capacity which slightly increases with the salinity increasing from 0 to 30%. For instance, the sorption capacities of PP-g-PBMA for diesel at 0, 10, 20, 30, and 40% salinity can reach 24.65, 24.94, 25.26, 25.70, and 25.07 g/g, respectively. The results suggest that there is no significant difference on sorption in deionized water and artificial seawater, which are similar with the results reported by Radetic et al. [51].

3.6. Reusability

Reusability is also an important indicator for evaluating the ability of oil-absorbing material to recover the absorbed oil. Good recycling performance of oil-absorbing material can reduce the cost of oil pollution treatment. The oil sorption capacity of PP-g-PBMA for three oils after eight sorption–desorption cycles are illustrated in Fig. 10. It can be seen that the oil sorption capacity continuously decreases during eight cycles. After four sorption/desorption cycles, the sorption capacity for soybean oil and lubricating oil decrease sharply. This phenomenon can be explained that the polymer structure may be destroyed and some fibers are collapsed during the vacuum process. After eight cycles, the losses in oil sorption capacity for diesel, soybean oil, and lubricating oil are 25.56, 36.42, and 33.11%, respectively. In addition, after eight cycles, the resulting PP-g-PBMA still exhibits better oil sorption capacity than PP for three oils. The results indicate that PP-g-PBMA shows excellent reusability capability.

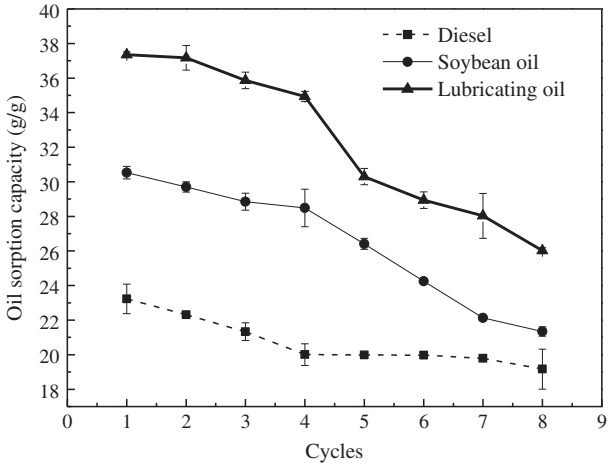

Fig. 10. Reusability of PP-g-PBMA for diesel, soybean oil, and lubricating oil.

4. Conclusions

In this study, PP-g-PBMA had been successfully prepared by suspension polymerization. The optimum preparation conditions were as follows: monomer concentration of 0.5 M, initiator concentration of 2.0 mM, and cross-linker dosage of 0.5%. The maximum sorption capacity of PP-g-PBMA for toluene, diesel, soybean oil, and lubricating oil can reach 18.65, 25.74, 33.56, and 38.90 g/g, respectively. The adsorption process was very fast. The oil absorbency was significantly influenced by stirring speed among environment conditions. In addition, PP-g-PBMA exhibited excellent reusability capability. The results suggested that PP-g-PBMA could be a candidate for the cleanup of spilled oil.

Acknowledgments

This work was funded by the National Natural Science Foundation of China (No. 41373097, 41073072), China. Postdoctoral Science Foundation funded project (No. 2013M541506), Program for Innovation Research Team in University (No. IRT13078).

References

[1] R.R. Huang, J. Hoinkis, Q. Hu, F. Koch, Treatment of dyeing wastewater by hollow fiber membrane biological reactor, Desalin. Water Treat. 11 (2009) 288–293.
[2] J. He, K. Yang, M. Dougherty, C. Li, Y. Wan, Removal of manganese from surface water with oxidants in supplement to natural manganese sand in Sinopec Shanghai Ltd, Desalin. Water Treat. 11 (2009) 245–257.
[3] D. Ceylan, S. Dogu, B. Karacik, S.D. Yakan, O.S. Okay, O. Okay, Evaluation of butyl rubber as sorbent material for the removal of oil and polycyclic aromatic hydrocarbons from seawater, Environ. Sci. Technol. 43 (2009) 3846–3852.
[4] S.E. Allan, B.W. Smith, K.A. Anderson, Impact of the deepwater horizon oil spill on bioavailable polycyclic aromatic hydrocarbons in Gulf of Mexico coastal waters, Environ. Sci. Technol. 46 (2012) 2033–2039.
[5] J.T. Wang, Y.A. Zheng, A.Q. Wang, Superhydrophobic kapok fiber oil-absorbent: Preparation and high oil absorbency, Chem. Eng. J. 213 (2012) 1–7.
[6] J.T. Korhonen, M. Kettunen, R.H.A. Ras, O. Ikkala, Hydrophobic nanocellulose aerogels as floating, sustainable, reusable, and recyclable oil absorbents, ACS Appl. Mater. Interfaces 3 (2011) 1813–1816.
[7] A.S. Franca, L.S. Oliveira, A.A. Nunes, C.C. Alves, Microwave assisted thermal treatment of defective coffee beans press cake for the production of adsorbents, Bioresour. Technol. 101 (2010) 1068–1074.
[8] H.M. Choi, R.M. Cloud, Natural sorbents in oil spill cleanup, Environ. Sci. Technol. 26 (1992) 772–776.
[9] O.K. Karakasi, A. Moutsatsou, Surface modification of high calcium fly ash for its application in oil spill clean up, Fuel 89 (2010) 3966–3970.
[10] O.K. Karakasi, A. Moutsatsou, By-products: Oil sorbents as a potential energy source, Waste Manage. Res. 31 (2013) 376–383.
[11] M. Roulia, K. Chassapis, C. Fotinopoulos, T. Savvidis, D. Katakis, Dispersion and sorption of oil spills by emulsifier-modified expanded perlite, Spill Sci. Technol. Bull. 8 (2003) 425–431.
[12] C. Teas, S. Kalligeros, F. Zanikos, S. Stournas, E. Lois, G. Anastopoulos, Investigation of the effectiveness of absorbent materials in oil spills clean up, Desalination 140 (2001) 259–264.
[13] A.V. Rao, N.D. Hegde, H. Hirashima, Absorption and desorption of organic liquids in elastic superhydrophobic silica aerogels, J. Colloid Interface Sci. 305 (2007) 124–132.
[14] S. Ibrahim, H.M. Ang, S.B. Wang, Removal of emulsified food and mineral oils from wastewater using surfactant modified barley straw, Bioresour. Technol. 100 (2009) 5744–5749.
[15] S. Ibrahim, S.B. Wang, H.M. Ang, Removal of emulsified oil from oily wastewater using agricultural waste barley straw, Biochem. Eng. J. 49 (2010) 78–83.
[16] S. Ibrahim, H.M. Ang, S.B. Wang, Adsorptive separation of emulsified oil in wastewater using biosorbents, Asia-Pacific J. Chem. Eng. 7 (2012) S216–S221.
[17] M. Likon, M. Remškar, V. Ducman, F. Švegl, Populus seed fibers as a natural source for production of oil super absorbents, J. Environ. Manage. 114 (2013) 158–167.
[18] K. Sathasivam, M.R.H.M. Haris, Adsorption kinetics and capacity of fatty acid-modified banana trunk fibers for oil in water, Water Air Soil Pollut. 213 (2010) 413–423.
[19] M.D. Teli, S.P. Valia, Acetylation of banana fibre to improve oil absorbency, Carbohydr. Polym. 92 (2013) 328–333.
[20] T.T. Lim, X. Huang, Evaluation of kapok (*Ceiba pentandra* (L.) Gaertn.) as a natural hollow hydrophobic-oleophilic fibrous sorbent for oil spill cleanup, Chemosphere 66 (2007) 955–963.

[21] M.A. Abdullah, A.U. Rahmah, Z. Man, Physicochemical and sorption characteristics of Malaysian *Ceiba pentandra* (L.) Gaertn. as a natural oil sorbent, J. Hazard. Mater. 177 (2010) 683–691.
[22] F. Ji, C.L. Li, X.Q. Dong, Y. Li, D.D. Wang, Separation of oil from oily wastewater by sorption and coalescence technique using ethanol grafted polyacrylonitrile, J. Hazard. Mater. 164 (2009) 1346–1351.
[23] H. Li, L.F. Liu, F.L. Yang, Hydrophobic modification of polyurethane foam for oil spill cleanup, Marine Pollut. Bull. 64 (2012) 1648–1653.
[24] X.M. Zhou, C.Z. Chuai, Synthesis and characterization of a novel high-oil-absorbing resin, J. Appl. Polym. Sci. 115 (2010) 3321–3325.
[25] V.K. Gupta, P.J.M. Carrott, M.M.L.R. Carrott, T.L. Suhas, Low-cost adsorbents: Growing approach to wastewater treatment—A review, Critical Rev. Environ. Sci. Technol. 39 (2009) 783–842.
[26] H.T. Zhu, S.S. Qiu, W. Jiang, D.X. Wu, C.Y. Zhang, Evaluation of electrospun polyvinyl chloride/polystyrene fibers as sorbent materials for oil spill cleanup, Environ. Sci. Technol. 45 (2011) 4527–4531.
[27] C. Lin, Y.J. Hong, A.H. Hu, Using a composite material containing waste tire powder and polypropylene fiber cut end to recover spilled oil, Waste Manage. 30 (2010) 263–267.
[28] H.Y. Li, W.F. Wu, M.M. Bubakir, H.B. Chen, X.F. Zhong, Z.X. Liu, Y.M. Ding, W.M. Yang, Polypropylene fibers fabricated via a needleless melt-electrospinning device for marine oil-spill cleanup, J. Appl. Polym. Sci. 131 (2014) 1–9.
[29] J. Zhao, C.F. Xiao, N.K. Xu, Evaluation of polypropylene and poly (butylmethacrylate-co-hydroxyethylmethacrylate) nonwoven material as oil absorbent, Environ. Sci. Pollut. Res. 20 (2013) 4137–4145.
[30] G.H. Jiang, R.B. Hu, X.H. Wang, X.G. Xi, R.J. Wang, Z. Wei, X. Li, B.L. Tang, Preparation of superhydrophobic and superoleophilic polypropylene fibers with application in oil/water separation, J. Text. I 104 (2013) 790–797.
[31] S.N. Li, J.F. Wei, Synthesis of novel polypropyleneacrylate fiber sorbent and evaluation of the sorption properties for organic contaminants from water surface, Desalin. Water Treat. 46 (2012) 359–365.
[32] J.T. Wang, Y.A. Zheng, A.Q. Wang, Preparation and properties of kapok fiber enhanced oil sorption resins by suspended emulsion polymerization, J. Appl. Polym. Sci. 127 (2013) 2184–2191.
[33] P.A. Kavaklı, N. Seko, M. Tamada, Radiation-induced graft polymerization of glycidyl methacrylate onto PE/PP nonwoven fabric and its modification toward enhanced amidoximation, J. Appl. Polym. Sci. 105 (2007) 1551–1558.
[34] J.T. Wang, Y.A. Zheng, A.Q. Wang, Coated kapok fiber for removal of spilled oil, Marine Pollut. Bull. 69 (2013) 91–96.
[35] A.M. Atta, S.H. El-Hamouly, A.M. AlSabagh, M.M. Gabr, Crosslinked poly(octadecene-alt-maleic anhydride) copolymers as crude oil sorbers, J. Appl. Polym. Sci. 105 (2007) 2113–2120.
[36] K. Sing, D. Everett, R. Haul, L. Moscou, R. Pierotti, J. Rouquerol, T. Siemieniewska, Reporting physisorption data for gas/solid systems with special reference to the determination of surface area and porosity, Pure Appl. Chem. 57 (1985) 603–619.
[37] Y. Chu, Q. Pan, Three-dimensionally macroporous Fe/C nanocomposites as highly selective oil-absorption materials, ACS Appl. Mater. Interfaces 4 (2012) 2420–2425.
[38] J.G. Gwon, S.Y. Lee, J.H. Kim, Thermal degradation behavior of polypropylene base wood plastic composites hybridized with metal (aluminum, magnesium) hydroxides, J. Appl. Polym. Sci. 131 (2014) 1–7.
[39] X.N. Shi, W.B. Wang, A.Q. Wang, Effect of surfactant on porosity and swelling behaviors of guar gum-g-poly(sodium acrylate-co-styrene)/attapulgite superabsorbent hydrogels, Colloids Surf., B: Biointerfaces 88 (2011) 279–286.
[40] Y. Feng, C.F. Xiao, Research on butyl methacrylate–lauryl methacrylate copolymeric fibers for oil absorbency, J. Appl. Polym. Sci. 101 (2006) 1248–1251.
[41] J. Wu, N. Wang, L. Wang, H. Dong, Y. Zhao, L. Jiang, Electrospun porous structure fibrous film with high oil adsorption capacity, ACS Appl. Mater. Interfaces 4 (2012) 3207–3212.
[42] D. Mysore, T. Viraraghavan, Y.C. Jin, Treatment of oily waters using vermiculite, Water Res. 39 (2005) 2643–2653.
[43] S. Chakraborty, S. Chowdhury, P.D. Saha, Adsorption of Crystal Violet from aqueous solution onto NaOH-modified rice husk, Carbohydr. Polym. 86 (2011) 1533–1541.
[44] I. Langmuir, The adsorption of gases on plane surfaces of glass, mica and platinum, J. Am. Chem. Soc. 40 (1918) 1361–1403.
[45] K.R. Hall, L.C. Eagleton, A. Acrivos, T. Vermeulen, Pore- and solid-diffusion kinetics in fixed-bed adsorption under constant-pattern conditions, Ind. Eng. Chem. Fundam. 5 (1966) 212–223.
[46] Y.S. Ho, G. McKay, Sorption of dye from aqueous solution by peat, Chem. Eng. J. 70 (1998) 115–124.
[47] F.A. Aisien, F.K. Hymore, R.O. Ebewele, Potential application of recycled rubber in oil pollution control, Environ. Monit. Assess. 85 (2003) 175–190.
[48] C. Lin, Y.J. Hong, A.H. Hu, Using a composite material containing waste tire powder and polypropylene fiber cut end to recover spilled oil, Waste Manage. 30 (2010) 263–267.
[49] J.T. Wang, Y.A. Zheng, A.Q. Wang, Kinetic and thermodynamic studies on the removal of oil from water using superhydrophobic kapok fiber, Water Environ. Res. 86 (2014) 360–365.
[50] Q.F. Wei, R.R. Mather, A.F. Fotheringham, Oil removal from used sorbents using a biosurfactant, Bioresour. Technol. 96 (2005) 331–334.
[51] M.M. Radetić, D.M. Jocić, P.M. Jovančić, Z.L. Petrović, H.F. Thomas, Recycled wool-based nonwoven material as an oil sorbent, Environ. Sci. Technol. 37 (2003) 1008–1012.